Soil Dynamics and Earthquake Engineering 179 (2024) 108524

Contents lists available at ScienceDirect

Soil Dynamics and Earthquake Engineering

journal homepage: www.elsevier.com/locate/soildyn

A ground motion intensity measure based on different spectral-shape types to predict nonlinear structural response in steel buildings

Victor Baca, Federico Valenzuela-Beltrán, Robespierre Chávez *, Edén Bojórquez, Alfredo Reyes-Salazar, Juan Bojórquez

Facultad de Ingeniería, Universidad Autónoma de Sinaloa, Culiacán, 80040, Sinaloa, Mexico

ARTICLE INFO

Keywords:
Ground motion intensity measure
Spectral shape
Nonlinear behavior
Structural response
Steel buildings

ABSTRACT

The selection of an appropriate intensity measure to assess the seismic performance in steel buildings is an important step to reduce uncertainty in the structural response. Hence, in this study, a scalar ground motion intensity measure able to increase the efficiency in the prediction of nonlinear behavior effects of steel structures subjected to earthquake ground motions named the generalized intensity measure I_{Npg} is analyzed. The intensity measure is based on a proxy of the spectral shape N_{pg}, where it can be defined by using different types of spectral shapes, such as those obtained with pseudo-acceleration, velocity, displacement, input energy, inelastic parameters and so on. This work shows the efficiency of the generalized intensity measure named I_{Npg} when the spectral parameters of pseudo-acceleration and velocity are used. Therefore, to improve the performance of the analyzed intensity measure, two engineering demand parameters, maximum inter-story drift and horizontal peak floor acceleration, of steel frames with 5, 10, 15 and 20 stories subjected to several narrow-band ground motions are estimated as a function of the spectral acceleration at first mode of vibration of the structure $Sa(T_1)$, which is commonly used in earthquake engineering and seismology, and with the two particular cases under study of the recently developed parameter related to the structural response known as I_{Npg}. In general, the intensity measure here studied is able to efficiently predict nonlinear structural demands on steel buildings under earthquake ground motions. Further, the analyzed intensity measure must be considered to estimate maximum inter-story drift and horizontal peak floor acceleration demand of multi-story buildings.

1. Introduction

The selection of appropriate ground motion intensity measures (IM) is crucial for accurately predicting structural response. Ground motion intensity measures serve as parameters that effectively decouple seismological and structural uncertainties. To achieve this desirable decoupling, intensity measures must primarily possess two characteristics: sufficiency and efficiency. Sufficiency refers to the fact that the structural response should depend solely on the intensity measure used, disregarding seismic source characteristics such as distance to the site of interest and earthquake magnitude. On the other hand, efficiency is defined as the ability to predict the response of structures subjected to earthquakes with low uncertainty. Therefore, selecting an efficient seismic intensity measure can significantly reduce the uncertainty associated with the seismic response of buildings subjected to ground motions.

The study of IMs has been a significant focus in the field of Earthquake Engineering since its inception. Recognizing the importance of identifying an appropriate IM, numerous studies have been conducted to determine a parameter that can effectively represent the ground motion potential of an earthquake [1–29]. Some studies have demonstrated the advantages of utilizing vector IMs for predicting structural response [6, 9]. However, it should be noted that despite the efficacy of vector IMs, their practical application is often limited. Consequently, the use of scalar IMs is more convenient as they provide a clearer understanding of the destructive potential of an earthquake. On another note, efforts to develop an appropriate IM have primarily focused on defining parameters associated with the spectral shape due to its correlation with structural response. In recent years, there has been an increasing number of studies advocating for the use of vector or scalar IMs based on spectral shape, as they have demonstrated good accuracy in predicting the maximum inter-story drift of buildings subjected to earthquakes [13,

* Corresponding author.
E-mail address: robespierre@uas.edu.mx (R. Chávez).

https://doi.org/10.1016/j.soildyn.2024.108524
Received 19 August 2023; Received in revised form 29 January 2024; Accepted 31 January 2024
Available online 10 February 2024

14].

Based on the above, the initial step involves finding a parameter that can accurately represent the spectral shape. Consequently, numerous vector and scalar IMs have been proposed, which effectively capture the spectral shape based on N_p, exhibiting a strong correlation with nonlinear structural response and various engineering demand parameters [13–15,30–33]. The parameter N_p is defined as the ratio between the geometrical mean spectral acceleration in the range T_1 and T_N, divided by $Sa(T_1)$. Furthermore, N_p has been successfully employed for record selection [34]. Several studies have demonstrated that the intensity measure I_{Np}, based on the spectral parameter of pseudo-acceleration proposed by Bojórquez and Iervolino [13], is one of the most efficient IMs available [30,33]. Several years later, in an effort to enhance the predictive capability of IMs, Bojórquez et al. [35] introduced the generalized intensity measure I_{Npg}. However, this work focused on proposing equations to quickly estimate the maximum inter-story drift using I_{Np}, rather than assessing the efficiency of I_{Npg}.

Many studies have been conducted to propose new IMs and analyze their efficiency, particularly focusing on the spectral shape in terms of acceleration. However, most of these studies have only examined the standard deviation of the maximum inter-story drift as an engineering demand parameter. It is important to extend the analysis and explore the relationship between intensity measures and maximum seismic responses using other engineering demand parameters and spectral shapes. In this regard, several studies have emphasized the need to consider additional engineering demand parameters such as peak floor acceleration, as it plays a crucial role in preventing damage to non-structural components, including hospital equipment [36,37].

This study aims to assess the efficiency of the generalized ground motion intensity measure I_{Npg} in the prediction of structural response in steel 3D buildings of different heights, comparing it with the commonly used IM known as $Sa(T_1)$. The main feature of I_{Npg} is to account for the effect of nonlinear behavior on the structural response, utilizing the spectral shape parameter N_{pg}. This IM improves the ability to predict the structural response considering a different range of periods and a wide range of spectral parameters taken from any type of spectrum as in the case of acceleration, velocity, displacement, input energy, inelastic parameters and so on. The objective is to demonstrate the potential of I_{Npg} to predict peak floor accelerations and maximum inter-story drift of multi-story 3D buildings, taking into account the spectral parameters of pseudo-acceleration and velocity.

2. The generalized spectral shape parameter N_{pg}

Recent studies suggest a strong correlation between the spectral shape and the structural response of buildings during seismic events. As a result, the earthquake engineering and seismology community has placed emphasis on the limitations of spectral acceleration in the first mode of vibration, known as $Sa(T_1)$. An illustrative example of this limitation is that $Sa(T_1)$ fails to provide spectral shape information beyond the period of the first mode of vibration, T_1. Such information may be crucial for nonlinear behavior or structures influenced primarily by higher modes, occurring before T_1. In the case of nonlinear shaking, the structure may be sensitive to different spectral values associated with a range of periods defined, from the fundamental period and a limit value of practical interest, say T_N.

Parameters such as $Sa_{avg}(T_1 \ldots T_N)$ or the area under the spectrum represent the spectra shape. Consequently, a specific value of $Sa_{avg}(T_1 \ldots T_N)$ or the area under the spectrum can be associated to different spectrum values between T_1 and T_N, signifying various spectral shapes. A useful enhancement involves normalizing $Sa_{avg}(T_1 \ldots T_N)$ with respect to $Sa(T_1)$. This normalization is the traditional definition of the spectral shape parameter known as N_p proposed by Bojórquez and Iervolino [13]. It is worth noting that the traditional N_p can be generalized to account for higher mode effects, as recommended by Bojórquez et al. [13,38]. For instance, Bojórquez et al. [34] employed the N_p parameter to consider higher mode effects and introduced a novel approach to select seismic records based on spectral shape using genetic algorithms. Furthermore, Bojórquez et al. [13,38] suggest that N_p can be calculated using a different range of periods. Generally, Bojórquez et al. [34] indicate that higher mode effects can be incorporated by modifying the N_p parameter evaluation, encompassing not only the period range from T_1 to T_N but also including a mode of interest (a period smaller than T_1) up to the final period T_N. For example, by assessing N_p from T_{2mode} to T_N (where T_{2mode} represents the period associated with the second mode of vibration of the structure). Additionally, alternative spectral shape parameters could be used in place of spectral acceleration. Consequently, a generalized form of N_p, denoted as N_{pg}, can be expressed as follows:

$$N_{pg} = \frac{S_{avg}(T_i, \ldots, T_N)}{S(T_j)} \tag{1}$$

In Eq. (1), $S(T_j)$ represents a spectral parameter extracted from some type of spectra, such as acceleration, velocity, displacement, input energy, inelastic parameters, and so on, at period T_j. $S_{avg}(T_i \ldots T_N)$ denotes the geometric mean of a specific spectral parameter within the period range from T_i and T_N. It's important to note that T_i and T_j can have different values. N_{pg} shares similarities with the traditional N_p definition [13], but it encompasses different types of spectra and a broader range of periods. Consequently, parameters like the traditional N_p or *SaRatio* [39] are specific cases of the generalized spectral shape parameter N_{pg}. When using the pseudo-acceleration spectrum, and $T_i = T_j = T_1$ (representing the period of the first mode of structural vibration), N_{pg} is equivalent to the traditional N_p and can also be denoted as N_{pSa}. It is expressed as follows:

$$N_{pSa} = N_p = \frac{Sa_{avg}(T_1, \ldots, T_N)}{Sa(T_1)} \tag{2}$$

Similarly, when $T_i = T_j = T_1$ and the velocity spectrum is utilized, N_{pg} is equivalent to N_{pVel}:

$$N_{pVel} = \frac{Vel_{avg}(T_1, \ldots, T_N)}{Vel(T_1)} \tag{3}$$

It is important to note that in Eqs. (2) and (3), the subscripts indicate the spectral parameter used. For example, in Eq. (2), the subscript *Sa* after N_p indicates the usage of pseudo acceleration as the spectral parameter. The information provided by I_{Npg} indicates that for one or *n* records with a mean I_{Npg} value close to one, a flat average spectrum is expected over the period range between T_1 and T_N. On the other hand, for a mean I_{Npg} value less than one, a negatively sloped average spectrum is expected, and a positive slope is associated with mean I_{Npg} values greater than one.

As an example, the mean value of N_{pSa} for a group of ordinary records in the period range $T_1 = 0.6$s to $T_N = 2T_1$ is 0.32, this value is associated with a negative slope. Fig. 1(a) illustrates the average spectrum of this record set. In the case of N_{pSa} values are larger than one, the spectra tend to increase beyond T_1. This can be observed for a set of narrow-band records, where the mean value of $N_p = 1.8$ for $T_1 = 1.2$s and $T_N = 2T_1$, resulting in an increasing acceleration zone in the average spectrum (see Fig. 1(b)).

In the case that velocity is used as a spectral parameter (see Fig. 2), the following observations can be made. When the N_{pg} values are close to one, the spectrum tends to be flat between T_1 and T_N, that is illustrated in Fig. 2(a) for the set of ordinary records. For instance, when the average value of $N_{pVel} = 0.95$ for $T_1 = 1.2$s and $T_N = 2.4$s, the average spectrum indicates that the velocities are similar in the considered zone. In Fig. 2 (b), the average spectrum for the set of narrow-band records is shown. In this case, the mean value N_{pVel} in the period range $T_1 = 1.2$ to $T_N = 2T_1$ is 1.44. Consequently, it can be observed that for N_{pg} values larger than one, regardless of the spectral parameter used, the spectra tend to increase beyond T_1.

Finally, as mentioned previously, it is possible to modify the initial

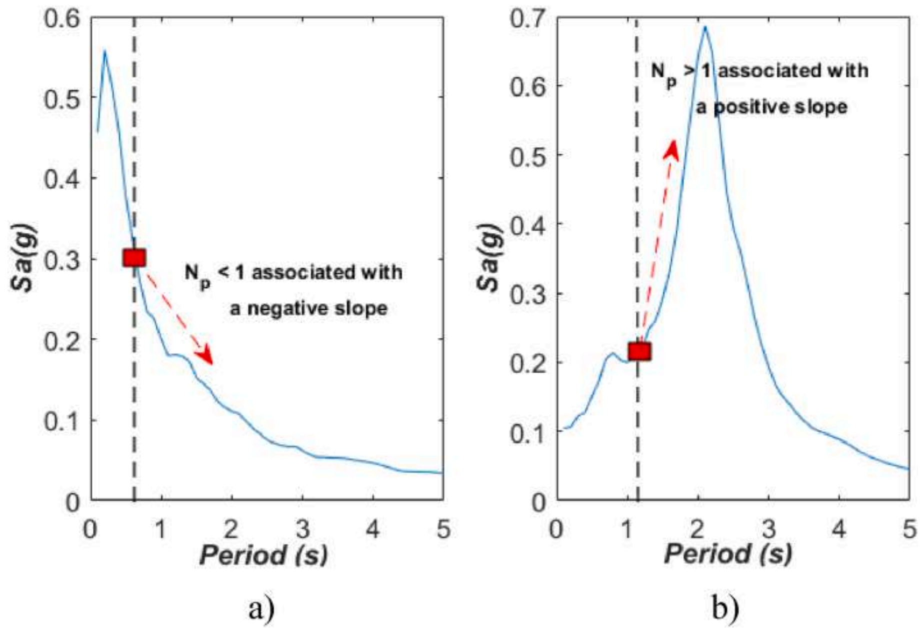

Fig. 1. Mean elastic response spectra for a set of: a) ordinary records with $N_p = 0.32$, b) narrow-band records with $N_p = 1.8$.

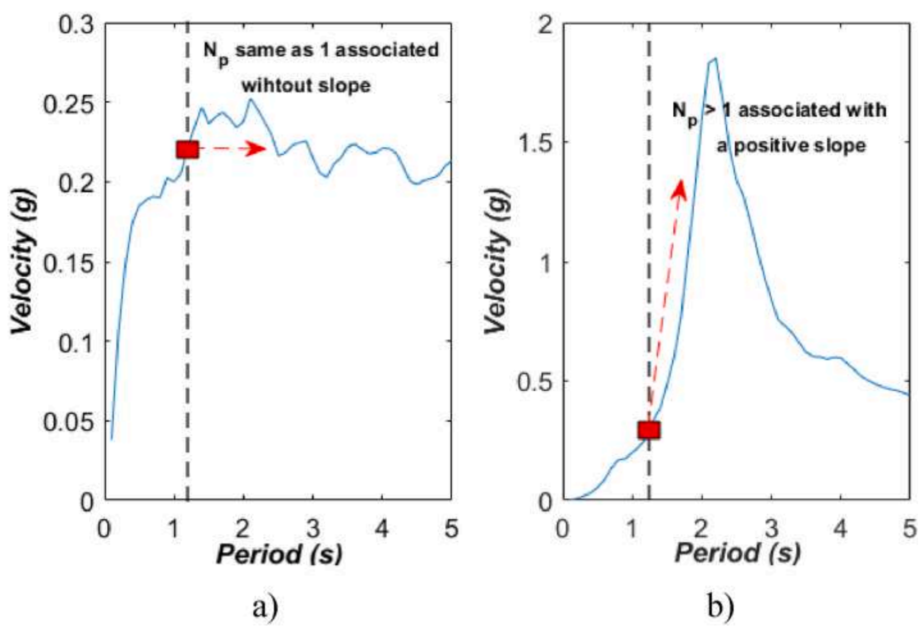

Fig. 2. Mean elastic response spectra for a set of: a) ordinary records with $N_p = 0.95$, b) narrow-band records with $N_p = 1.44$.

period T_1 and the final period T_N in the N_{pg} parameter to account for higher mode effects, as suggested by Bojórquez et al. [13,34,38]. Therefore, N_{pg} is not limited to a specific range, and the spectral parameter can be taken from any response spectrum demand, such as velocity, displacement, seismic energy, etc. [13,38].

3. I_{Npg} ground motion intensity measure

The main characteristic of the ground motion intensity measure I_{Npg} is its ability to capture the effects of nonlinear behavior in predicting structural response. It builds upon the traditional intensity measure I_{Np} proposed by Bojórquez and Iervolino [13]. The key distinction between these intensity measures lies in the fact that the generalized I_{Npg} [35] incorporates a wide range of spectral parameters derived from various types of spectra, such as acceleration, velocity, displacement, input energy, inelastic parameters, and so on. In contrast, the traditional I_{Np} solely utilizes pseudo-acceleration as the spectral parameter. Consequently, the generalized I_{Npg} is defined as follows:

$$I_{Npg} = S(T_1)N_{pg}^{\alpha} \tag{4}$$

In Eq. (4), the value of α needs to be determined through regression analysis. $S(T_1)$ represents a spectral parameter extracted from any type of spectrum, such as acceleration, velocity, displacement, input energy, inelastic parameters, and so on, specifically at the first mode of vibration. The generalized N_{pg} is defined in Eq. (1). For the purpose of this study, only pseudo-acceleration and velocity spectral parameters are taken into account. Therefore, when substituting these parameters into Eq. (4), the following equations are obtained:

$$I_{NpSa} = Sa(T_1)\left[\frac{Sa_{avg}(T_1, \ldots, T_N)}{Sa(T_1)}\right]^{\alpha} \quad (5)$$

$$I_{NpVel} = Vel(T_1)\left[\frac{Vel_{avg}(T_1, \ldots, T_N)}{Vel(T_1)}\right]^{\alpha} \quad (6)$$

When examining Eqs. (5) and (6), it is important to note that the subscripts indicate the spectral parameter employed. For instance, in Eq. (6), the subscript *Vel* after I_{Np} signifies the usage of velocity as the spectral parameter. By observing Equation (5), several key points can be noted when pseudo acceleration is utilized *1)* the traditional intensity measure I_{Np} proposed by Bojórquez and Iervolino [13] represents a specific case of the generalized I_{Npg}; *2)* the spectral acceleration at the first mode of vibration becomes a specific case when α is equal to zero; *3)* $Sa_{avg}(T_1, \ldots, T_N)$ also corresponds to a specific case when $\alpha = 1$.

Based on the analyses conducted by Bojórquez and Iervolino [13] and Buratti [30], it has been suggested that the optimal values of α for the traditional I_{Np} or I_{NpSa} are approximately 0.4. Additionally, Buratti [30]demonstrated that this intensity measure is more effective in predicting the seismic response of structures compared to several other IMs found in the literature. As for I_{NpVel}, it is necessary to conduct optimization studies to determine the optimal values of α that minimize the uncertainty in predicting the structural response. However, the main objective of this study is to showcase the potential of the intensity measures I_{NpSa} and I_{NpVel} with an α value equal to 0.4 employed for both cases.

It should be noted that the generalized I_{Npg} assigns distinct weights to the contributions of spectral parameters beyond the first mode, in contrast to the spectral value at T_1. Additionally, the generalized I_{Npg} can be utilized in the development of probabilistic seismic hazard analysis, similar to the traditional I_{Np}, as demonstrated by Bojórquez and Iervolino [13].

4. Structural steel-framed buildings

In this research, four moment-resisting steel frames were utilized to evaluate the efficiency of two specific cases of I_{Npg}, based on acceleration and velocity. These three-dimensional structures depict typical steel buildings in Mexico, varying in height with 5, 10, 15, and 20 stories. All buildings share the same plan distribution, consisting of four 7-m bays in the North-South direction and three 7-m bays in the East-West direction, with a consistent story height of 3 m. Fig. 3 provides a visual representation of the three-dimensional structures. The frames were designed according to the Complementary Technical Norms for Seismic Design (NTCDS-2017) of the Mexico City Building Code (MCBC) [40]. The structures under consideration are office buildings situated in the soft soil zone of Mexico City with a dominant period of 2 s. Table 1 presents the dynamic characteristics of each building, including the structural vibration period (T_1), the second mode period (T_{2m}), and the modal participation mass ratio of the first two vibration modes. T_1 and T_{2m} refer to periods corresponding to the modes of vibration in the two orthogonal directions of each studied building.

To assess the efficiency of the generalized intensity measure I_{Npg}, the responses of four steel buildings were estimated by modeling them by complex 3D MDOF frames. The nonlinear analyses were performed with the Ruaumoko 3D Software [41] where a 3 % viscous damping assumption was applied to develop the Rayleigh damping matrix. The Newmark constant average acceleration method was employed within the Ruaumoko environment to solve the differential equation systems. The nonlinear dynamic analysis accounted for large displacement effects (P-Δ and P-d), utilizing an integration time step of 0.001 s. The vertical structural members were modeled as beam-columns, while horizontal members were modeled as beams. A rigid panel zone was considered at the intersection of beams and beam columns. The hysteretic behavior of the members was modeled as bilinear, incorporating 3 % post-elastic stiffness. The interaction between axial loads and bending moments was defined by the interaction surface proposed by Chen and Atsuta [42].

5. Ground motion records

The efficiency of ground motion intensity measures was calculated using 30 pairs narrow-band ground motions recorded at sites in the Lake Zone of Mexico City, which experienced significant structural damage during the well-known 1985 Mexican earthquake. Additionally, these sites have consistently exhibited higher levels of peak ground acceleration (*PGA*) and velocity (*PGV*), and soil periods of 2 s are quite common within the Lake Zone. Table 2 provides a summary of the main properties of the recorded data. It is worth noting that the North-South and East-West components of each selected record were employed

Table 1
Dynamic characteristics of structural models.

Structural Model	Number of stories	Height (m)	Vibration Period (sec)		Modal participation mass ratio	
			T_1	T_{2m}	T_1	T_{2m}
F5	5	15	1.08	0.89	0.82	0.80
F10	10	30	1.52	1.36	0.74	0.72
F15	15	45	1.91	1.59	0.77	0.76
F20	20	60	2.19	1.86	0.74	0.73

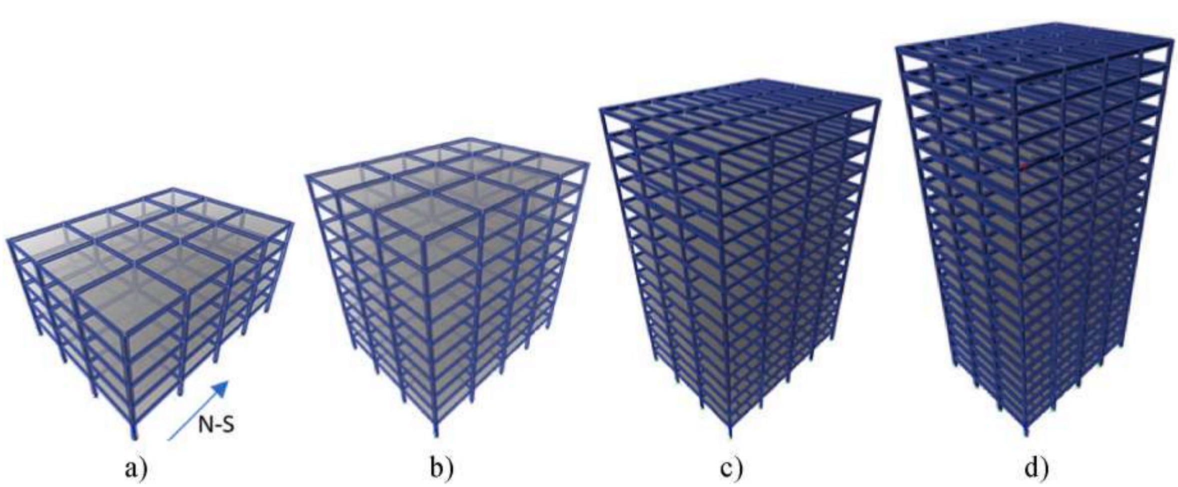

Fig. 3. Three-dimensional view of the selected structural models: a) F5, b) F10, c) F15 and d) F20.

Table 2
Narrow-band earthquake ground motions.

Record	Date	Station	Moment magnitud	*PGA* (cm/s^2)	*PGV* (cm/s)	Epicentral Distance (km)	*Duration (s)*
1	19/09/1985	SCT	8.1	178.0	59.5	366	34.8
2	21/09/1985	Tlahuac deportivo	7.6	48.7	14.6	323	39.9
3	25/04/1989	Alameda	6.9	45.0	15.6	293	37.8
4	25/04/1989	Garibaldi	6.9	68.0	21.5	294	65.5
5	25/04/1989	SCT	6.9	44.9	12.8	289	65.8
6	25/04/1989	Sector Popular	6.9	45.1	15.3	286	79.4
7	25/04/1989	Tlatelolco TL08	6.9	52.9	17.3	295	56.6
8	25/04/1989	Tlatelolco TL55	6.9	49.5	17.3	293	50.0
9	14/09/1995	Alameda	7.3	39.3	12.2	303	53.7
10	14/09/1995	Garibaldi	7.3	39.1	10.6	303	86.8
11	14/09/1995	Liconsa	7.3	30.1	9.62	286	60.0
12	14/09/1995	Plutarco Elías Calles	7.3	33.5	9.37	298	77.8
13	14/09/1995	Sector Popular	7.3	34.3	12.5	295	101.2
14	14/09/1995	Tlatelolco TL08	7.3	27.5	7.8	304	85.9
15	14/09/1995	Tlatelolco TL55	7.3	27.2	7.4	303	68.3
16	09/10/1995	Cibeles	7.5	14.4	4.6	536	85.5
17	09/10/1995	CU Juárez	7.5	15.8	5.1	537	97.6
18	09/10/1995	C. urbano P. Juárez	7.5	15.7	4.8	537	82.6
19	09/10/1995	Córdoba	7.5	24.9	8.6	537	105.1
20	09/10/1995	Liverpool	7.5	17.6	6.3	537	104.5
21	09/10/1995	Plutarco Elías Calles	7.5	19.2	7.9	539	137.5
22	09/10/1995	Sector Popular	7.5	13.7	5.3	540	98.4
23	09/10/1995	Valle Gómez	7.5	17.9	7.18	541	62.3
24	11/01/1997	CU Juárez	6.9	16.2	5.9	379	61.1
25	11/01/1997	C. urbano P. Juárez	6.9	16.3	5.5	379	85.7
26	11/01/1997	García Campillo	6.9	18.7	6.9	381	57.0
27	11/01/1997	Plutarco Elías Calles	6.9	22.2	8.6	381	76.7
28	11/01/1997	Est. # 10 Roma A	6.9	21.0	7.76	380	74.1
29	11/01/1997	Est. # 10 Roma B	6.9	20.4	7.1	380	81.6
30	11/01/1997	Tlatelolco TL08	6.9	16.0	7.2	383	57.5

simultaneously for nonlinear dynamic time history analysis. The scaling was done based on the square root of the sum of the squares (SRSS) rule, as described in Eq. (7):

$$S_{SRSS}(T) = \sqrt{S_{NS}^2(T) + S_{EW}^2(T)} \tag{7}$$

where S_{NS} and S_{EW} are the response spectrum ordinates associated with a

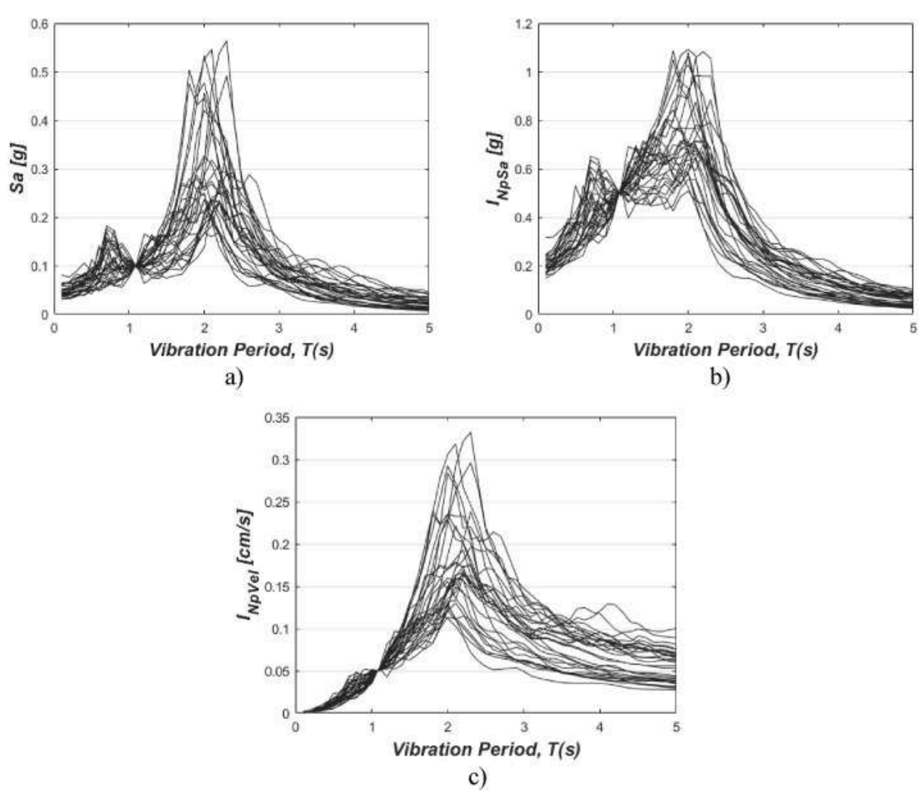

Fig. 4. SRSS scaled response spectrum in the fundamental period of the structural model F5 ($T = 1.08$ s) for a specific intensity value and the IM considered: a) *Sa* (T_1), b) I_{NpSa} and c) I_{NpVel}.

period T and an IM, for the N-S and E-W components, respectively. Therefore, the term S_{SRSS} represents the combined spectrum ordinates in each orthogonal direction using the SRSS rule. For the seismic analyses, the ground motions were scaled using $Sa(T_1)$, I_{NpSa} and I_{NpVel} in the fundamental period of vibration of the structure T_1 (N-S direction), with an α value set tat 0.4 for both particular cases of the generalized intensity measure I_{Npg}. Fig. 4 illustrates the SRSS scaled response spectrum at the fundamental period of the structural model F5 for specific intensity values of 0.1 g, 0.5 g, and 0.05 cm/s for $Sa(T_1)$, I_{NpSa} and I_{NpVel}, respectively.

As is widely recognized, scaling seismic records to perform incremental dynamic analysis involves scaling the records to various intensity levels. Therefore, it is important to emphasize that the intensity values, for which the spectra presented in Fig. 4 were scaled, were randomly selected from the results obtained in this study. The spectra depicted in Fig. 4 represent only a portion of the scaling process, as they specifically pertain to one level of scaling for a structural model and the IMs under consideration in this study. The spectra shown in Fig. 4 were not utilized in the incremental dynamic analyses. On the other hand, both scaled orthogonal components of the selected records were input simultaneously to perform nonlinear time history analyses.

6. Efficiency indicators

The efficiency of an IM can be evaluated based on its capacity to offer an accurate and dependable representation of earthquake effects. It is essential to acknowledge that different IMs may be better suited for specific purposes, underscoring the importance of comprehending their characteristics and limitations. The evaluation of an IM efficiency can be accomplished through the utilization of statistical measures.

These statistical parameters or efficiency indicators allow determining whether resources are used optimally and whether the results obtained are satisfactory. Standard deviation, correlation coefficient, and coefficient of determination are among the commonly employed parameters to evaluate efficiency in seismic intensity measurements.

Standard deviation is a statistical measure that quantifies the dispersion or variability of a dataset in relation to its mean. Regarding the efficiency of an IM, the standard deviation can be utilized to assess the consistency and accuracy of the obtained results. On the other hand, the correlation coefficient is a statistical measure that quantifies the extent of the relationship or association between two variables. Denoted as r, it takes a value ranging between -1 and 1. This measure is an important tool in data analysis as it enables the evaluation of the relationship between variables and determines whether a significant association exists between them.

Another parameter utilized in IM analysis is the coefficient of determination, also known as R^2. This statistical measure is employed in regression analysis to evaluate the goodness of fit between a regression model and the observed data. The coefficient of determination ranges between 0 and 1 and indicates the proportion of the total variance in the dependent variable that is explained by the regression model. In simpler terms, it signifies how closely the data points align with the fitted regression model.

Hence, the efficiency of an IM can be evaluated by employing statistical measures such as standard deviation, correlation coefficient, and coefficient of determination. These efficiency indicators allow for an assessment of consistency, precision, and relationship with other variables.

7. Incremental dynamic analysis and efficiency study

To evaluate the seismic performance of selected steel frames, incremental dynamic analysis was conducted [43]. Incremental dynamic analysis is a reliable tool widely used in civil engineering [44–46]. It involves performing a series of nonlinear time-history analyses using a set of ground motion records scaled at various intensity levels. In incremental dynamic analysis, it is necessary to define an intensity measure that characterizes the severity of the seismic input, as well as an appropriate engineering demand parameter to assess the structural response.

The seismic performance of buildings was assessed using a set of 30 pairs ground motion records consistent with the seismic hazard of the area where the models are located, scaled at different $Sa(T_1)$, I_{NpSa} and I_{NpVel} values, with the aid of Ruaumoko 3D software [41]. The ground motion records were scaled to induce significant non-linearity in the structures, resulting in a substantial increase in the number of analysis operations and the accuracy of the results. Twenty scaling levels were considered for each of the selected IMs. Given the diverse approaches used by IM to evaluate intensity, the selected intensity ranges differ among these IMs. In the case of $Sa(T_1)$ and I_{NpSa}, their intensity ranges coincide because they both depend on pseudo-acceleration. Furthermore, efforts were made to ensure that the demand thresholds reached were similar in the selected intensity range. On the other hand, I_{NpVel} depends on another spectral parameter, the spectral velocity, resulting in a different intensity range. Nevertheless, the goal was to achieve comparable demand thresholds within this range of intensity.

7200 non-linear structural dynamic analyses were conducted to identify critical parameters such as maximum inter-story drift and peak floor acceleration demands for the selected steel frames and intensity measures used in the study. This extensive dataset, derived from simulations, offers a more comprehensive understanding of structural responses to different intensity measures.

8. Efficiency study

Efficiency studies of IMs usually focus on the maximum inter-story drift as the demand parameter. Nevertheless, various studies have emphasized the significance of considering peak floor acceleration in buildings to prevent damage to nonstructural components, including hospital equipment [36,37]. Consequently, in this study, two engineering demand parameters, the maximum inter-story and peak floor acceleration, have been selected to facilitate a comparison of efficiency among the chosen IMs.

Based on the dynamic analyses performed in the previous section, the maximum inter-story drift and peak floor acceleration demands for each structure were obtained. After the standard deviation, correlation and regression coefficient of the natural logarithm of the peak engineering demand parameters for the buildings subjected to a set of narrow-band earthquake ground motions were obtained to evaluate the efficiency of $Sa(T_1)$ and the two particular cases of generalized intensity measure I_{Npg}, as defined by Eqs. (5) and (6). It should be noted that each case of the generalized intensity measure I_{Npg} needs to be optimized in order to accurately predict engineering demand parameters for buildings and enhance efficiency.

In this study, the maximum inter-story drift and peak floor acceleration demands were obtained for both the N-S and E-W directions. However, only the results for the N-S direction are presented, as the results in the other direction exhibit substantial similarity.

Fig. 5 presents the incremental dynamic analysis of selected IMs in terms of peak floor acceleration demands for frame model F15 under the selected narrow-band ground motions. The vertical axis represents the maximum peak floor acceleration, while the horizontal axis corresponds to intensity levels for $Sa(T_1)$, I_{NpSa} and I_{NpVel}, respectively. From Fig. 5 (a), a clear relationship between $Sa(T_1)$ and peak floor acceleration demands can be observed. However, the uncertainty in predicting peak demands using spectral acceleration tends to increase with higher intensity levels of the earthquake ground motion. On the other hand, Fig. 5 (b) and (c) illustrate that the uncertainty in predicting structural response for larger intensity levels is lower when using I_{NpSa} and I_{NpVel}, this is also observable in Table 3.

Table 3 illustrates the standard deviation by intensity level for the IMs selected and the steel frame F15. In addition, it shows the median

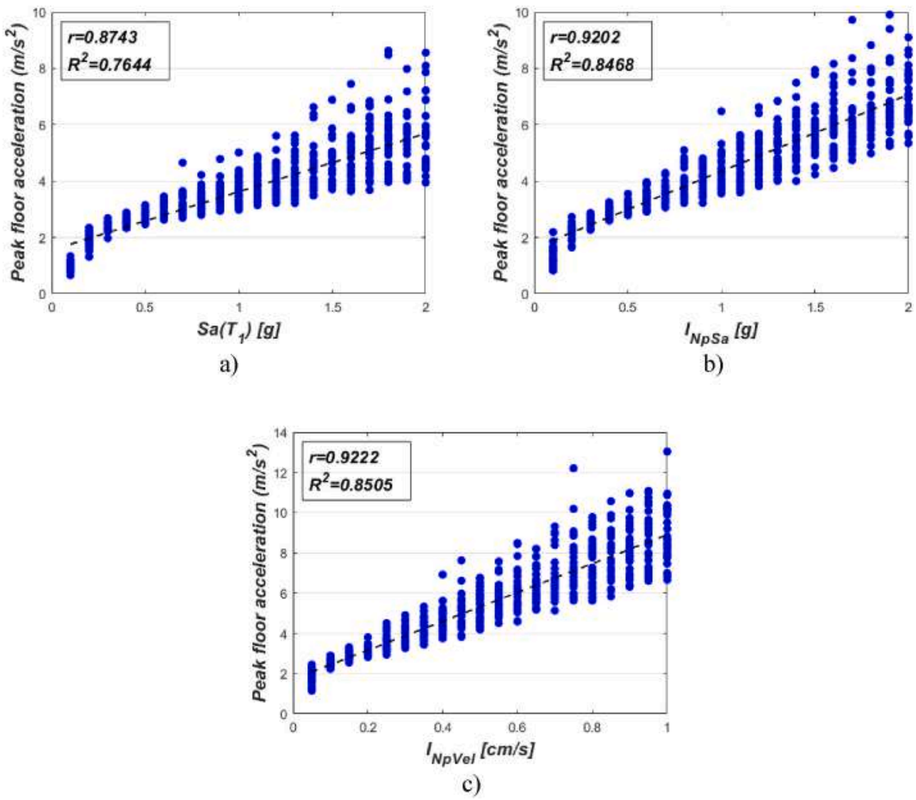

Fig. 5. Incremental dynamic analysis in terms of peak floor acceleration for steel frame F15 under narrow-band motions using: a) $Sa(T_1)$, b) I_{NpSa} and c) I_{NpVel}.

Table 3
Standard deviation and Median peak floor acceleration value by intensity level for steel frame F15 using $Sa(T_1)$, I_{NpSa} and I_{NpVel}.

$Sa(T_1)$			I_{NpSa}			I_{NpVel}		
Intensity level (g)	Standard deviation	Median peak floor acceleration value (m/s^2)	Intensity level (g)	Standard deviation	Median peak floor acceleration value (m/s^2)	Intensity level (cm/s)	Standard deviation	Median peak floor acceleration value (m/s^2)
0.1	0.1465	0.9866	0.1	0.2399	1.3514	0.05	0.1953	1.8170
0.2	0.1220	1.9220	0.2	0.1108	2.2455	0.1	0.0529	2.5307
0.3	0.0582	2.3828	0.3	0.0568	2.6001	0.15	0.0652	2.9084
0.4	0.0548	2.6082	0.4	0.0625	2.8900	0.2	0.0692	3.1737
0.5	0.0683	2.8147	0.5	0.0601	3.0650	0.25	0.1042	3.5338
0.6	0.0823	2.9746	0.6	0.0881	3.3344	0.3	0.1089	3.8377
0.7	0.1134	3.1256	0.7	0.0983	3.5671	0.35	0.1147	4.1254
0.8	0.1010	3.2724	0.8	0.1306	3.8505	0.4	0.1290	4.6703
0.9	0.1127	3.5263	0.9	0.1075	4.0391	0.45	0.1527	5.0480
1	0.1297	3.6376	1	0.1271	4.3657	0.5	0.1310	5.3819
1.1	0.1313	3.9047	1.1	0.1371	4.5043	0.55	0.1232	5.6614
1.2	0.1409	3.9849	1.2	0.1334	4.8661	0.6	0.1616	6.1329
1.3	0.1539	4.1545	1.3	0.1401	5.1161	0.65	0.1100	6.2553
1.4	0.1715	4.3984	1.4	0.1406	5.4557	0.7	0.1479	6.6972
1.5	0.1512	4.6036	1.5	0.1323	5.6522	0.75	0.1839	7.1641
1.6	0.1812	4.7686	1.6	0.1585	5.9791	0.8	0.1579	7.4033
1.7	0.1742	5.0494	1.7	0.1535	6.0689	0.85	0.1502	7.8366
1.8	0.1973	5.2739	1.8	0.1292	6.4336	0.9	0.1384	8.0751
1.9	0.1808	5.3480	1.9	0.1438	6.7085	0.95	0.1663	8.4912
2	0.2045	5.6406	2	0.1347	6.8797	1	0.1538	8.9896

peak floor acceleration value associated with said standard deviation. This table provides a clearer understanding that, as the intensity level increases, the uncertainty in the prediction of the structural response increases for the IMs selected, which is reflected in a higher standard deviation. However, the standard deviation for I_{NpSa} and I_{NpVel} is not as high as that presented for $Sa(T_1)$. Therefore, reduced uncertainty in structural response is an indicator of the efficiency of an IM.

Other parameters utilized to assess the efficiency of IMs include correlation and determination coefficients. This study employed the least squares regression method (LSRM) to fit a linear model to the data and be able to obtain these parameters. LSRM is a common method for estimating coefficients in linear regression equations describing the relationship between one or more quantitative independent variables and a dependent variable. These parameters and the regression line are shown in Fig. 5.

The correlation coefficient values illustrated in Fig. 5 show a very strong correlation between intensity level and response parameters for I_{NpSa} and I_{NpVel}, while a strong correlation is observed for $Sa(T_1)$. In addition, the highest regression value is observed for the particular cases of the generalized intensity measure I_{Npg}, whereas the regression value decreases for $Sa(T_1)$. This indicates the potential of I_{NpSa} and I_{NpVel} in predicting the structural response compared to the commonly used $Sa(T_1)$. The correlation coefficient and regression values in this example were obtained considering the range of intensities shown in Fig. 5 (horizontal axis). Later in this section, the correlation coefficient and regression values for all IMs and steel frames examined in this study will be presented.

The peak floor acceleration values obtained from dynamic analyses, shown in Fig. 5, exhibit a tendency to concentrate at the upper levels for the steel frame F15. Similar analyses were conducted for the steel frames F5, F10, and F20, confirming the concentration of peak floor acceleration at the upper levels for the steel frames studied in this research.

The incremental dynamic analysis for the selected IMs and frame model F15, under narrow-band ground motions, is presented in Fig. 6. In this case, the maximum inter-story drift is utilized as the demand parameter. Therefore, in Fig. 6, the vertical axis represents the maximum inter-story drift, while the horizontal axis corresponds to intensity levels for $Sa(T_1)$, I_{NpSa} and I_{NpVel}, respectively.

Fig. 6(a) presents a trend similar to that observed in Fig. 5(a). Specifically, a clear relationship between $Sa(T_1)$ and drift demands is evident for low-intensity levels, whereas a significant increase in uncertainty is observed when using spectral acceleration to predict peak demands at moderate and high-intensity levels. For example, when $Sa(T_1)$ values are less than 0.5g, spectral acceleration proves to be an excellent intensity measure since the prediction uncertainty is negligible, as the seismic response of the steel structure is nearly linear elastic. However, for steel frame F15 and an intensity value of 1.4g, the maximum inter-story drifts range from 0.024 to 0.077, indicating substantial uncertainty and the limitations of $Sa(T_1)$ in predicting the seismic response of this structure at high levels of nonlinear behavior. Moreover, the median maximum inter-story drift associated with this intensity value is equal to 0.04.

Clearly, it is necessary to employ efficient intensity measures that possess better predictive capability for the structural response, such as the generalized I_{Npg}, as evidenced in Fig. 6(b) and (c). As stated above for small intensity values, $Sa(T_1)$ is an excellent predictor of the structural response, however, for higher intensities, the range of maximum inter-story drift demands at a specific level of I_{NpSa} or I_{NpVel} is not as extensive as in the case of $Sa(T_1)$. To illustrate this point, one approach is to determine the median maximum inter-story drifts for each intensity level and then compare the standard deviation of each IM at the same median maximum inter-story drift value.

For example, the median maximum inter-story drifts equal to 0.04 for the steel frame F15 corresponds to a peak drift range of 0.026 to 0.061 for an I_{NpSa} value of 1.0g. Similarly, an I_{NpVel} value that causes the same median maximum inter-story drift for steel frame F15 is 0.4 cm/s, with peak drifts ranging from 0.027 to 0.071. In general, the stability in predicting maximum inter-story drifts is superior when using I_{NpSa} and I_{NpVel} for steel frame F15, as indicated in Table 4. Additionally, Table 5 presents the dispersion for a median peak floor acceleration value of 4 m/s^2 for steel frame F15 and the selected intensity measures.

Tables 4 and 5 show the dispersion of results, focusing on a particular

Table 4
Standard deviation for the median maximum inter-story drifts value approximately equal to 0.04 for the steel frame F15.

IM	Intensity level	Drifts		Standard deviation
		Minimum	Maximum	
$Sa(T_1)$	1.4 g	0.024	0.077	0.3033
I_{NpSa}	1.0 g	0.026	0.061	0.2350
I_{NpVel}	0.4 cm/s	0.027	0.071	0.2241

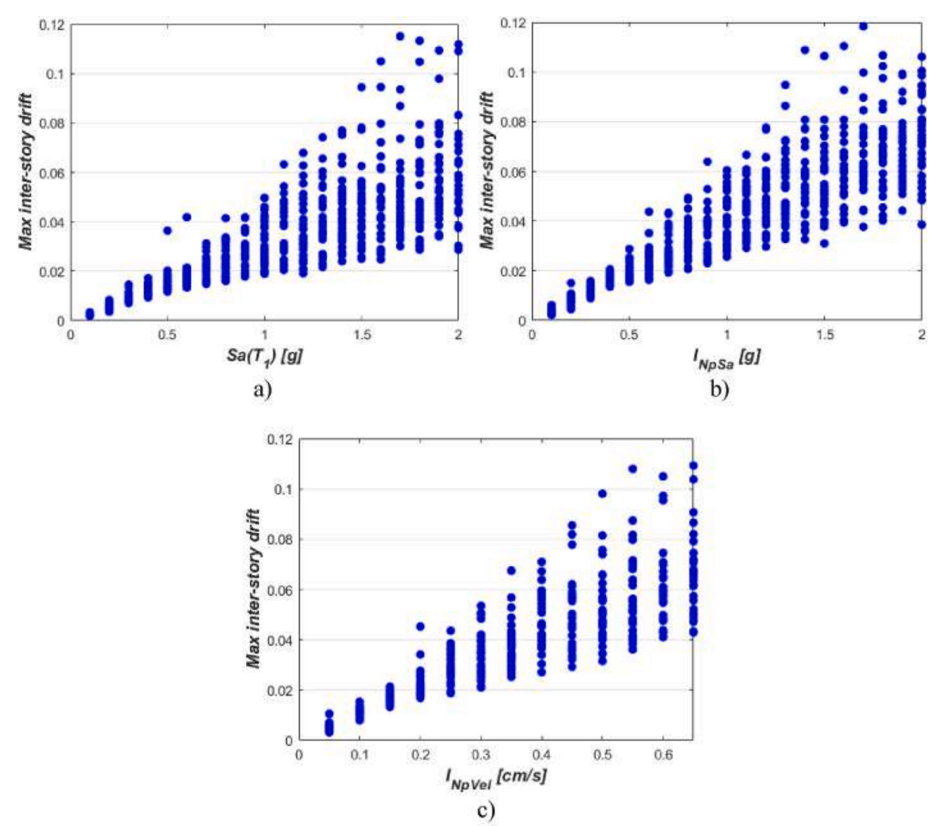

Fig. 6. Incremental dynamic analysis in terms of maximum inter-story drift for steel frame F15 under narrow-band motions using: a) $Sa(T_1)$, b) I_{NpSa} and c) I_{NpVel}.

Table 5
Standard deviation for the median peak floor acceleration value approximately equal to 4 m/s^2 for the steel frame F15.

IM	Intensity level	Floor acceleration (m/s^2)		Standard deviation
		Minimum	Maximum	
$Sa(T_1)$	1.3 g	3.21	5.62	0.1409
I_{NpSa}	0.9 g	3.22	4.80	0.1075
I_{NpVel}	0.35 cm/s	3.44	5.33	0.1147

median engineering demand parameter value and a specific structural model. However, a more comprehensive analysis of the results obtained for all the studied buildings and the considered intensity measures is provided in the subsequent discussion.

Then, when comparing the same median maximum inter-story drift value, it is evident from Table 4 that the range of maximum inter-story drifts is narrower for I_{NpSa} and I_{NpVel} compared to when $Sa(T_1)$ is used. This results in a reduction in the standard deviation values to 23 % and 26 % for I_{NpSa} and I_{NpVel}, respectively. Similarly, when comparing the same median peak floor acceleration value (Table 5), a reduction in the standard deviation of 24 % and 19 % can be observed for I_{NpSa} and I_{NpVel}, respectively. These results indicate the advantages of utilizing either of the two I_{Npg} cases mentioned above in comparison to using spectral acceleration at the first mode of vibration.

Consequently, the results suggest that large uncertainty is associated with the spectral acceleration as intensity measure. In contrast, the generalized intensity measure I_{Npg} demonstrates superior efficiency in characterizing the seismic response of buildings under narrow-band motions as observed in the selected cases examined in this study. However, given the diverse approaches used by IM to evaluate intensity, it is recommended to compare them within a limited intensity range for more accurate and representative conclusions. The lower limit of this range was defined as the point where buildings exhibit non-linear behavior, while the upper limit was selected at an intensity level where the maximum demand parameter was approximately the same for a given building and the considered intensity measures.

For example, Fig. 7 illustrates the incremental dynamic analysis conducted on the steel frame F10. The horizontal axis of the figure represents the intensities range considered for the different IMs, while the vertical axis corresponds to the demand parameter, specifically the peak floor acceleration. The results shown in Fig. 7 indicate a very strong correlation between the intensity level and response parameters for the particular cases of generalized intensity measure I_{Npg}, while a strong correlation is observed for the $Sa(T_1)$. On the other hand, the regression value is highest, there is less dispersion in the structural response, when I_{NpSa} and I_{NpVel} are used, however, the dispersion increases when $Sa(T_1)$ is used as IM, it is shown in the Fig. 7.

Table 6 presents the correlation coefficient values for maximum inter-story drift and peak floor acceleration for the buildings and IMs considered in this study. The table reveals the potential for predicting the structural response of the two particular cases of the generalized intensity measure I_{Npg}. This is because the correlation coefficient values for I_{NpSa} and I_{NpVel} show a very strong correlation between the intensity level and response parameters, while for $Sa(T_1)$ a strong correlation is obtained. However, despite the similarity of correlation coefficient values for the two particular cases of I_{Npg}, it is evident that the strongest correlation is achieved when using I_{NpSa}. This suggests that I_{NpSa} is the most efficient parameter for predicting the structural response.

The regression values for maximum inter-story drift and peak floor acceleration of steel frames and IMs considered in this study are shown in Table 7. The table demonstrates that the regression values exhibit a similar trend as the correlation coefficient. Notably, the highest regression value is observed for the two particular cases of the generalized intensity measure I_{Npg}. This indicates that there is less dispersion in the structural response when I_{NpSa} and I_{NpVel} are used. Moreover, this trend remains consistent regardless of the engineering demand parameter. However, although the regression values are quite similar for the two particular cases of I_{Npg}, the least dispersion occurs when I_{NpSa} is employed.

By examining Tables 6 and 7, it is evident that I_{NpSa} and I_{NpVel} are

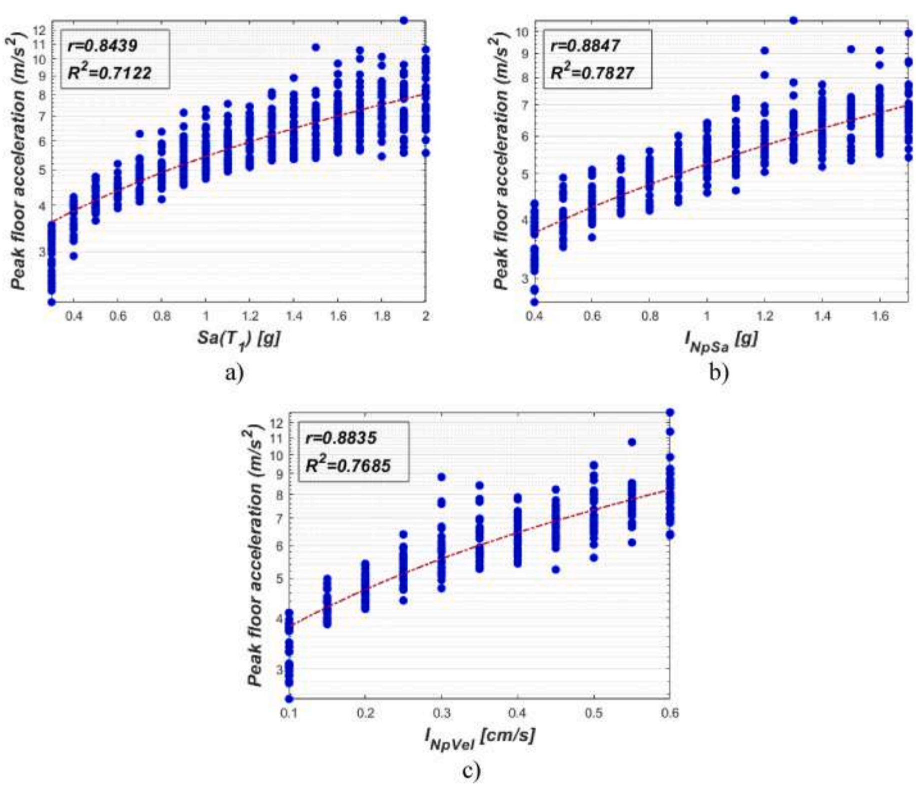

Fig. 7. Incremental dynamic analysis in terms of peak floor acceleration for steel frame F10 under narrow-band motions using: a) $Sa(T_1)$, b) I_{NpSa} and c) I_{NpVel}.

Table 6
Correlation coefficient (ρ) for maximum inter-story drift and peak floor acceleration.

IM	Maximum inter-story drift				Peak floor acceleration			
	F5	F10	F15	F20	F5	F10	F15	F20
$Sa(T_1)$	0.7521	0.7417	0.7470	0.7822	0.8359	0.8439	0.7560	0.6685
I_{NpSa}	0.8194	0.8400	0.8252	0.8333	0.8610	0.8847	0.8604	0.8107
I_{NpVel}	0.8243	0.8379	0.8072	0.8295	0.8730	0.8835	0.8577	0.6984

Table 7
Coefficient of determination (R^2) for maximum inter-story drift and peak floor acceleration.

IM	Maximum inter-story drift				Peak floor acceleration			
	F5	F10	F15	F20	F5	F10	F15	F20
$Sa(T_1)$	0.5658	0.5502	0.5580	0.6119	0.6988	0.7122	0.5715	0.4469
I_{NpSa}	0.6714	0.7056	0.6810	0.6944	0.7413	0.7827	0.7403	0.6573
I_{NpVel}	0.6795	0.7023	0.6503	0.6881	0.7261	0.7685	0.7310	0.4877

more efficient in predicting the structural response compared to $Sa(T_1)$. Nevertheless, an analysis of the tables reveals that, when considering the correlation coefficient and regression as efficiency indicators, I_{NpSa} could be considered the most efficient IM for a large number of the buildings analyzed in this study.

Figs. 8-11 illustrate the standard deviation of the logarithms of the medians of demands for the steel Frames F5, F10, F15, and F20, subjected the set of the narrow-band ground motions. These figures compare the dispersion of structural demands for each of the considered IM. For example, utilizing the data from Table 3, Fig. 10(b) was developed, displaying the standard deviation of the mean values of peak floor acceleration for the F15 frame. It is important to note that, due to the intensity values in Table 3 are not directly comparable between the different IMs, a decision was made to opt for a range of structural demand values (ranging from 3 to 5.5 m/s^2 for Frame F15, as illustrated in Fig. 10(b)) and compute the corresponding standard deviation on these values. To illustrate, consider a median peak floor acceleration value of 5 m/s^2 for Frame F15, marked with a circle in Fig. 10(b). Referring to the data in Table 3, the standard deviation associated to that level of peak floor acceleration is approximately 0.1754, 0.1370, and 0.1497 for $Sa(T_1)$, I_{NpSa}, and I_{NpVel}, respectively. This procedure was replicated for each of the demand values shown in Fig. 10(b). The same methodology was applied to all the frames under investigation, resulting in the obtaining Fig. 8-11.

The results of the standard deviation of the IMs associated with the median values of maximum inter-story drift and peak floor acceleration for the low-rise steel Frame F5 are presented in Fig. 8(a) and (b). These figures clearly demonstrate that the intensity measure I_{NpSa} exhibits the best performance across the entire range of median maximum inter-story drift and peak floor acceleration values. On the other hand, both I_{NpVel} and $Sa(T_1)$ display similar performance throughout the entire range for the selected engineering demand parameters. Therefore, it is advisable to use I_{NpSa} as the intensity measure for predicting the structural response of low-rise steel Frames with T_1 less than 1.08 s.

For steel Frames F10 and F15 (Figs. 9 and 10), it is illustrated that across the entire range of median maximum inter-story drift values, the two particular cases of the generalized intensity measure I_{Npg} are better candidates for predicting the structural response. I_{NpSa} and I_{NpVel} exhibit a lower standard deviation compared to $Sa(T_1)$. However, in the specific case of the steel frame F10 (Fig. 9(a)), it can be observed that across the entire range of median maximum inter-story drift values, I_{NpSa} performs better than I_{NpVel}. On the other hand, for steel Frame F15 (Fig. 10(a)), the two particular cases of generalized intensity measure I_{Npg} exhibit similar performance. Additionally, the efficiency of the IMs for median values of peak floor acceleration is shown in Fig. 9(b) and 10(b) for mid-rise steel Frames. From Fig. 9(b), it can be seen that the performance of I_{NpSa} and I_{NpVel} is better than $Sa(T_1)$ for most median value ranges for steel Frames F10. In the case of steel Frames F15, the superiority in terms of efficiency

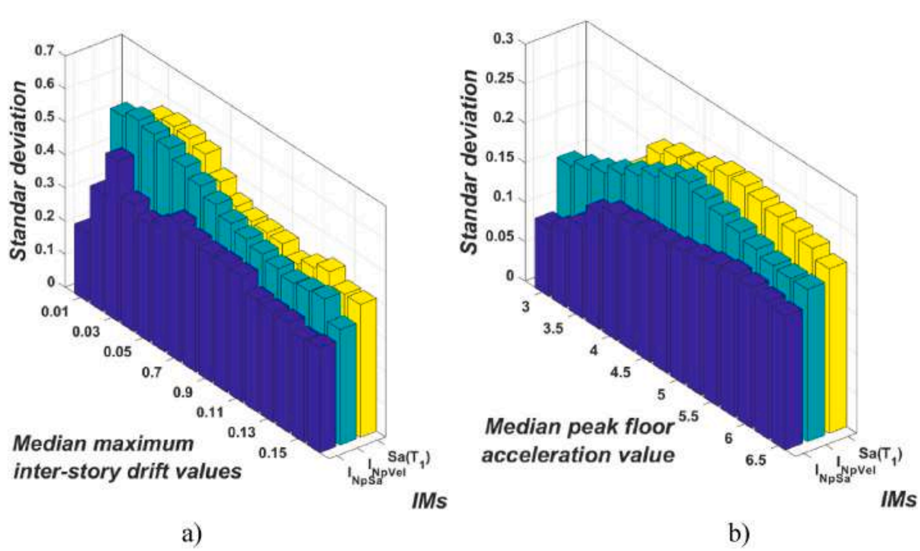

Fig. 8. Standard deviation between selected IMs and steel Frame F5: a) for median maximum inter-story drift values and b) for median peak floor acceleration values.

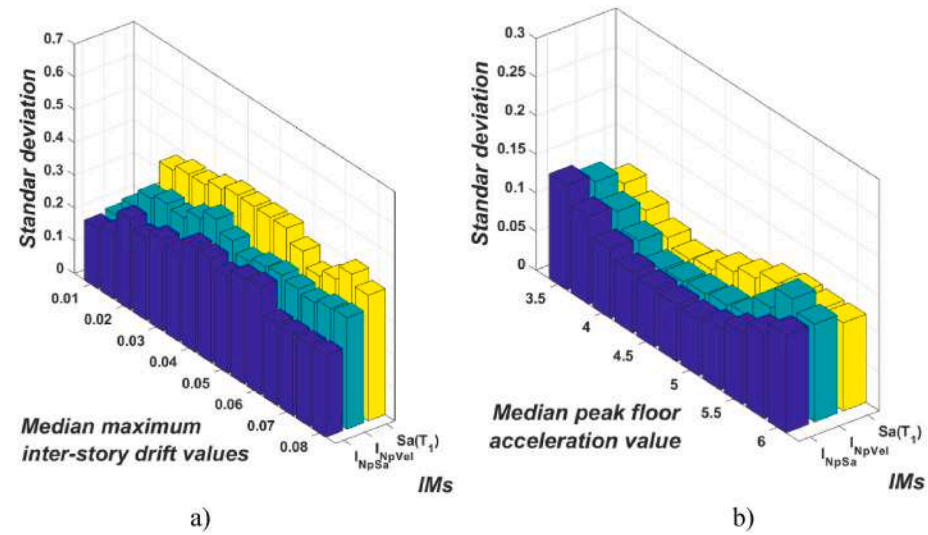

Fig. 9. Standard deviation between selected IMs and steel Frame F10: a) for median maximum inter-story drift values and b) for median peak floor acceleration values.

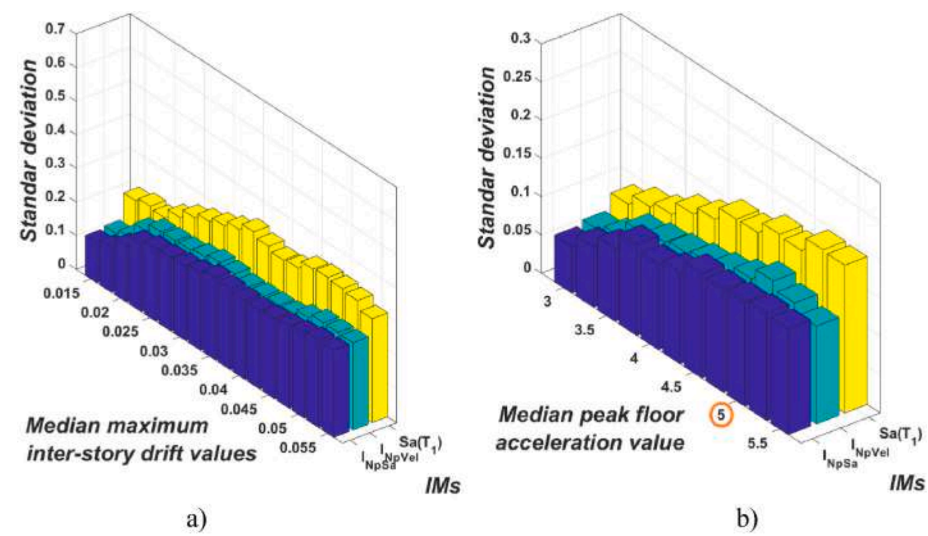

Fig. 10. Standard deviation between selected IMs and steel Frame F15: a) for median maximum inter-story drift values and b) for median peak floor acceleration values.

of the particular cases of the generalized intensity measure I_{Npg} over $Sa(T_1)$ can be seen more clearly. I_{NpSa} and I_{NpVel} exhibit a lower standard deviation for most of the mean values, as depicted in Fig. 10(b). Only in a median value of peak floor acceleration, the performance of $Sa(T_1)$ is similar to that of I_{NpSa}. Therefore, for mid-rise steel Frames, either of the two particular cases of the generalized intensity measure I_{Npg} could be used to predict the structural response.

When analyzing the results of the high-rise steel Frame F20, the ranking of the IMs is not clear across the entire range of median peak floor acceleration values. From Fig. 11(b), it can be observed that $Sa(T_1)$ demonstrates the best performance for lower median peak floor acceleration values. However, for larger values, the particular cases of the generalized intensity measure I_{Npg} are more efficient. On the other hand, in Fig. 11(a), the superiority of the particular cases of the generalized intensity measure I_{Npg} in predicting the seismic response is more evident. Specifically, I_{NpVel} exhibits the best performance with lower standard deviation in a significant portion of the range of median maximum inter-story drift values.

The above figures demonstrate that the particular cases of the generalized intensity measure I_{Npg} are good candidates to be used in the prediction of the structural response. However, for most of the four buildings studied here, the efficiency of I_{NpSa} is comparable to, and in some cases even surpasses, that of I_{NpVel}. Importantly, it should be noted that the efficiency of I_{NpSa} is consistently superior to the traditional $Sa(T_1)$ measure, nearly in all cases.

9. Conclusion

This study focuses on analyzing the efficiency of the generalized seismic intensity measure I_{Npg}, specifically for the particular cases of I_{NpSa} and I_{NpVel} with an α value equal to 0.4. The main characteristic of this IM is its ability to account for nonlinear behavior in predicting the structural response. Additionally, the generalized I_{Npg} incorporates the spectral shape through the parameter N_{pg}. This parameter offers the flexibility of using a wide range of spectral shapes derived from various types of spectra, such as acceleration, velocity, displacement, input energy, inelastic parameters, and more.

The efficiency of two particular cases of the generalized ground

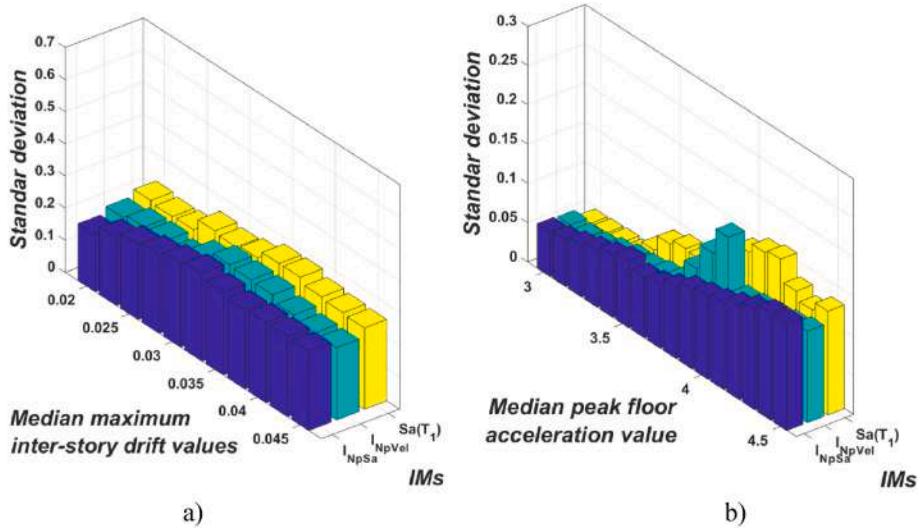

Fig. 11. Standard deviation between selected IMs and steel Frame F20: a) for median maximum inter-story drift values and b) for median peak floor acceleration values.

motion intensity measure I_{Npg} in predicting the seismic response of steel frame buildings under narrow-band motions was compared with the spectral acceleration at the first mode of vibration. The results obtained for the correlation coefficient reveal that the correlation between the intensity level and the response parameter is very strong for the selected IMs. Nevertheless, the two specific cases of the generalized intensity measure I_{Npg} show a stronger correlation compared to when $Sa(T_1)$ is used. Additionally, the regression analysis indicates a lower dispersion in the structural response when considering I_{NpSa} and I_{NpVel}. On the other hand, it is generally observed that the standard deviation of the natural logarithm of the maximum inter-story drift and peak floor acceleration is lower for the two specific cases of the generalized intensity measure I_{Npg}.

In conclusion, it was found that the uncertainty in predicting maximum inter-story drift and peak floor acceleration demands of the buildings was significantly reduced when utilizing the two specific cases of the generalized intensity measure I_{Npg}. Moreover, the efficiency of the intensity measure I_{NpSa} was generally superior compared to I_{NpVel}. Therefore, the generalized ground motion intensity measure proves to be the preferred option for predicting maximum inter-story drift and peak floor accelerations for the steel-framed buildings considered in this study. However, further studies are necessary to explore and select different types of spectral shapes to define I_{Npg}, especially for high-rise buildings.

In conclusion, it was found that the uncertainty in predicting maximum inter-story drift and peak floor acceleration demands of the buildings was significantly reduced when utilizing the two specific cases of the generalized intensity measure I_{Npg}. Moreover, the efficiency of the intensity measure I_{NpSa} was generally superior compared to I_{NpVel}. Therefore, the generalized ground motion intensity measure proves to be the preferred option for predicting maximum inter-story drift and peak floor accelerations for the steel-framed buildings considered in this study. However, further studies are necessary to explore and select different types of spectral shapes to define I_{Npg}, optimize α values in I_{Npg}, and account for soil structure interaction, especially for high-rise buildings.

Statement of originality

The originality of this study, compared to existing ones, lies in the assessment of the efficiency of the generalized intensity measure I_{Npg} of three-dimensional steel frames of low to medium height. This assessment is achieved through the use of spectral parameters such as pseudo-acceleration and velocity. To achieve this objective, several nonlinear dynamic analyses were conducted to obtain the seismic response of these frames. The response was evaluated in relation to different engineering demand parameters, including maximum interstory drift and maximum floor acceleration. The results of this investigation strongly indicate the superior efficiency of the generalized seismic intensity measure I_{Npg} when compared to the commonly employed intensity measure $Sa(T_1)$.

CRediT authorship contribution statement

Victor Baca: Writing – original draft, Methodology, Conceptualization. **Federico Valenzuela-Beltrán:** Formal analysis, Data curation. **Robespierre Chávez:** Writing – review & editing, Methodology, Conceptualization. **Edén Bojórquez:** Visualization, Investigation. **Alfredo Reyes-Salazar:** Validation, Supervision. **Juan Bojórquez:** Software, Resources.

Declaration of competing interest

The authors declare that they have no known competing financial interests or personal relationships that could have appeared to influence the work reported in this paper.

Data availability

Data will be made available on request.

Acknowledgments

The financial support granted by the Universidad Autónoma de Sinaloa through the grant PROFAPI 2022, as well as for providing the resources and the enabling environment to carry out this research, is highly appreciated. We also extend our gratitude to the two anonymous reviewers for their careful evaluations and valuable feedback, which significantly contributed to enhancing the quality of the paper.

References

[1] Housner GW. Spectrum intensities of strong-motion earthquakes. In: Proceedings of the symposium on earthquake and blast effects on structures. Los Angeles, California: Earthquake Engineering Research Institute; Jun. 1952. p. 20–36.

[2] Arias A. A measure of earthquake intensity," *seismic Design for nuclear power plants*. 1970. p. 438–83.

[3] Housner GW. Measures of severity of earthquake ground shaking. In: U.S. Conference on earthquake engineering. Earthquake Engineering Research Institute; 1975.
[4] Aptikaev FF. On the correlations of MM intensity with parameters of ground shaking. In: The 7th European conference on earthquake engineering. Grecia: Atenas; 1982.
[5] Von-Thun JL, Roehm LH, Scott GA, Wilson JA. Earthquake ground motions for design and analysis of dams, 20. Geotechnical special publication; 1988. p. 463–81.
[6] Shome N. Probabilistic seismic demand analysis of nonlinear structures. Stanford University; 1999.
[7] Cordova PP, Deierlein GG, Mehanny SSF, Cornell CA. Development of a two-parameter seismic intensity measure and probabilistic assessment procedure. In: The second U.S.-Japan workshop on performance-based earthquake engineering methodology for reinforce concrete building structures. Hokkaido: Sapporo; 2001. p. 187–206.
[8] Mehanny SS, Cordova PP. Development of a two-parameter seismic intensity measure and probabilistic design procedure. J Eng Appl Sci 2004;51(2):233–52.
[9] Baker JW, Cornell CA. A vector-valued ground motion intensity measure consisting of spectral acceleration and epsilon. Earthq Eng Struct Dynam Aug. 2005;34(10):1193–217. https://doi.org/10.1002/eqe.474.
[10] Tothong P, Luco N. Probabilistic seismic demand analysis using advanced ground motion intensity measures. Earthq Eng Struct Dynam Oct. 2007;36(13):1837–60. https://doi.org/10.1002/eqe.696.
[11] Riddell R. On ground motion intensity indices. Earthq Spectra Feb. 2007;23(1):147–73. https://doi.org/10.1193/1.2424748.
[12] Mehanny SSF. A broad-range power-law form scalar-based seismic intensity measure. Eng Struct Jul. 2009;31(7):1354–68. https://doi.org/10.1016/j.engstruct.2009.02.003.
[13] Bojórquez E, Iervolino I. Spectral shape proxies and nonlinear structural response. Soil Dynam Earthq Eng Jul. 2011;31(7):996–1008. https://doi.org/10.1016/j.soildyn.2011.03.006.
[14] Bojórquez E, Iervolino I, Reyes-Salazar A, Ruiz SE. Comparing vector-valued intensity measures for fragility analysis of steel frames in the case of narrow-band ground motions. Eng Struct Dec. 2012;45:472–80. https://doi.org/10.1016/j.engstruct.2012.07.002.
[15] Minas S, Galasso C, Rossetto T. Preliminary investigation on selecting optimal intensity measures for simplified fragility analysis of mid-rise RC buildings. In: 2nd European conference on earthquake engineering and seismology (2ECEES), istanbul, Turkey; Aug. 2014.
[16] Kostinakis K, Athanatopoulou A, Morfidis K. Correlation between ground motion intensity measures and seismic damage of 3D R/C buildings. Eng Struct Jan. 2015;82:151–67. https://doi.org/10.1016/j.engstruct.2014.10.035.
[17] Yakhchalian M, Nicknam A, Amiri GG. Optimal vector-valued intensity measure for seismic collapse assessment of structures. Earthq Eng Eng Vib Mar. 2015;14(1):37–54. https://doi.org/10.1007/s11803-015-0005-6.
[18] Kazantzi AK, Vamvatsikos D. Intensity measure selection for vulnerability studies of building classes. Earthq Eng Struct Dynam Dec. 2015;44(15):2677–94. https://doi.org/10.1002/eqe.2603.
[19] Tsantaki S, Adam C, Ibarra LF. Intensity measures that reduce collapse capacity dispersion of P-delta vulnerable simple systems. Bull Earthq Eng Mar. 2017;15(3):1085–109. https://doi.org/10.1007/s10518-016-9994-4.
[20] Morelli F, Laguardia R, Faggella M, Piscini A, Gigliotti R, Salvatore W. Ground motions and scaling techniques for 3D performance based seismic assessment of an industrial steel structure. Bull Earthq Eng Mar. 2018;16(3):1179–208. https://doi.org/10.1007/s10518-017-0244-1.
[21] Amirsardari A, Rajeev P, Lumantarna E, Goldsworthy HM. Suitable intensity measure for probabilistic seismic risk assessment of non-ductile Australian reinforced concrete buildings. Bull Earthq Eng Jul. 2019;17(7):3753–75. https://doi.org/10.1007/s10518-019-00632-1.
[22] Dávalos H, Miranda E. Filtered incremental velocity: a novel approach in intensity measures for seismic collapse estimation. Earthq Eng Struct Dynam Oct. 2019;48(12):1384–405. https://doi.org/10.1002/eqe.3205.
[23] Yakhchalian M, Ghodrati Amiri G. A vector intensity measure to reliably predict maximum drift in low- to mid-rise buildings. Proceedings of the Institution of Civil Engineers - Structures and Buildings Jan. 2019;172(1):42–54. https://doi.org/10.1680/jstbu.17.00040.
[24] Yakhchalian M, Yakhchalian M, Yakhchalian M. Reliable fragility functions for seismic collapse assessment of reinforced concrete special moment resisting frame structures under near-fault ground motions. Struct Des Tall Special Build Jun. 2019;28(9):e1608. https://doi.org/10.1002/tal.1608.
[25] Pinzón LA, Vargas-Alzate YF, Pujades LG, Diaz SA. A drift-correlated ground motion intensity measure: application to steel frame buildings. Soil Dynam Earthq Eng May 2020;132:106096. https://doi.org/10.1016/j.soildyn.2020.106096.
[26] Amiri M, Yakhchalian M. Performance of intensity measures for seismic collapse assessment of structures with vertical mass irregularity. Structures Apr. 2020;24:728–41. https://doi.org/10.1016/j.istruc.2020.01.038.
[27] Yakhchalian M, Yakhchalian M, Asgarkhani N. An advanced intensity measure for residual drift assessment of steel BRB frames. Bull Earthq Eng Mar. 2021;19(4):1931–55. https://doi.org/10.1007/s10518-021-01051-x.
[28] Durucan C, Şahin H, Durucan AR. A new ground motion intensity measure for short period reinforced concrete structures subjected to near-fault pulse-like ground motions. Mech Base Des Struct Mach Apr. 2023;51(4):2004–19. https://doi.org/10.1080/15397734.2021.1886114.
[29] Rong X-L, Yang J, Jun L, Zhang Y-X, Zheng S-S, Dong L. Optimal ground motion intensity measure for seismic assessment of high-rise reinforced concrete structures. Case Stud Constr Mater Jul. 2023;18:e01678. https://doi.org/10.1016/j.cscm.2022.e01678.
[30] Buratti N. A comparison of the performances of various ground-motion intensity measures. In: The 15th world conference on earthquake engineering. Lisbon: Portugal; Sep. 2012.
[31] Modica A, Stafford PJ. Vector fragility surfaces for reinforced concrete frames in Europe. Bull Earthq Eng Aug. 2014;12(4):1725–53. https://doi.org/10.1007/s10518-013-9571-z.
[32] Málaga-Chuquitaype C, Bougatsas K. Scalar and vector-IM-based drift hazard estimations for steel buildings with alternative framing configurations. In: 16th world conference on earthquake engineering, santiago Chile; Jan. 2017.
[33] Rajabnejad H, Hamidi H, Naseri SA, Abbaszadeh MA. Effect of intensity measures on the response of a 3D-structure under different ground motion duration. Int J Eng Oct. 2021;34(10):2219–37. https://doi.org/10.5829/ije.2021.34.10a.04.
[34] Bojórquez E, Reyes-Salazar A, Ruiz SE, Bojórquez J. A new spectral shape-based record selection approach using Np and genetic algorithms. Math Probl Eng 2013;2013:1–9. https://doi.org/10.1155/2013/679026.
[35] Bojórquez E, Baca V, Bojórquez J, Reyes-Salazar A, Chávez R, Barraza M. A simplified procedure to estimate peak drift demands for mid-rise steel and R/C frames under narrow-band motions in terms of the spectral-shape-based intensity measure I. Eng Struct Nov. 2017;150:334–45. https://doi.org/10.1016/j.engstruct.2017.07.046.
[36] Kehoe BE, Freeman SA. A critique of procedures for calculating seismic design forces for nonstructural elements. In: Seminar on seismic design, retrofit, and performance of nonstructural components. USA: CA; 1998. p. 57–70.
[37] Horne P, Burton H. Investigation of code seismic force levels for hospital equipment. In: The ATC-29-2 seminar on seismic design, performance and retrofit of nonstructural components in critical facilities, Newport Beach, California; Oct. 2003.
[38] Bojorquez E, et al. Prediction of hysteretic energy demands in steel frames using vector-valued IMs. Steel Compos Struct Sep. 2015;19(3):697–711. https://doi.org/10.12989/scs.2015.19.3.697.
[39] Eads L, Miranda E, Lignos D. Spectral shape metrics and structural collapse potential. Earthq Eng Struct Dynam Aug. 2016;45(10):1643–59. https://doi.org/10.1002/eqe.2739.
[40] Reglamento de Construcciones de la Ciudad de México. Normas Técnicas Complementarias para Diseño por Sismo. Gaceta Oficial de La Ciudad de México; Dec. 2017.
[41] Carr AJ. RUAUMOKO inelastic dynamic analysis program. Cantenbury, Nueva Zelanda: DepQartament of Civil Engineering, University of Cantenbury; 2011.
[42] Chen WF, Atsuta T. Interaction equations for biaxially loaded sections. J Struct Div May 1972;98(5):1035–52. https://doi.org/10.1061/JSDEAG.0003223.
[43] Vamvatsikos D, Cornell CA. Incremental dynamic analysis. Earthq Eng Struct Dynam Mar. 2002;31(3):491–514. https://doi.org/10.1002/eqe.141.
[44] Deierlein GG, Reinhorn AM, Willford MR. Nonlinear structural analysis for seismic Design. 2010.
[45] Nicknam A, Mosleh A, Hamidi Jamnani H. Seismic performance evaluation of urban bridge using static nonlinear procedure, case study: hafez bridge. Procedia Eng 2011;14:2350–7. https://doi.org/10.1016/j.proeng.2011.07.296.
[46] Baharmast H, Razmyan S, Yazdani A. Approximate incremental dynamic analysis using reduction of ground motion records. Int J Eng 2015;28(2):190–7. https://doi.org/10.5829/idosi.ije.2015.28.02b.04.